International Journal of Electrical and Computer Engineering (IJECE)
Vol. 4, No. 4, August 2014, pp. 561~572
ISSN: 2088-8708

A Novel Retinal Blood Vessel Segmentation Algorithm using Fuzzy segmentation

Razieh Akhavan*, Karim Faez**
* Department of Computer Engineering, Qazvin Branch, Islamic Azad University, Qazvin, Iran
** Electrical Engineering Department, Amirkabir University of Technology, Tehran, Iran

Article Info

Article history:

Received May 12, 2014
Revised Jun 23, 2014
Accepted Jul 8, 2014

Keyword:

Adaptive fuzzy switching Median filter
Blood vessel segmentation
Fuzzy vessel segmentation
Modified morphological operations
Vessel centerline detection

ABSTRACT

Assessment of blood vessels in retinal images is an important factor for many medical disorders. The changes in the retinal vessels due to the pathologies can be easily identified by segmenting the retinal vessels. Segmentation of retinal vessels is done to identify the early diagnosis of the disease like glaucoma, diabetic retinopathy, macular degeneration, hypertensive retinopathy and arteriosclerosis. In this paper, we propose an automatic blood vessel segmentation method. The proposed algorithm starts with the extraction of blood vessel centerline pixels. The final segmentation is obtained using an iterative region growing method that merges the binary images resulting from centerline detection part with the image resulting from fuzzy vessel segmentation part. In this proposed algorithm, the blood vessel is enhanced using modified morphological operations and the salt and pepper noises are removed from retinal images using Adaptive Fuzzy Switching Median filter. This method is applied on two publicly available databases, the DRIVE and the STARE and the experimental results obtained by using green channel images have been presented and compared with recently published methods. The results demonstrate that our algorithm is very effective method to detect retinal blood vessels.

Corresponding Author:

Razieh Akhavan,
Department of Computer Engineering,
Islamic Azad University, Gazvin branch, Gazvin, Iran
Email: R.akhavan.a@gmail.com

1. INTRODUCTION

The diagnosis of the fundus image is widely used in many medical diagnoses. Image segmentation [1] in the fundus image is the important factor for identifying the retinal pathology. The analysis of the human retina helps the ophthalmologists to identify the retinal disease. The disease such as the diabetes, hypertension and arteriosclerosis affect the retina and cause the changes in the retinal blood vessels [2]. The changes in the blood vessel and the retinal pathology can be identified by first segmenting the retinal vessels and by proper analysis of the retinal blood vessels.

Automatic segmentation of retinal vessels is important for early diagnosis of eye diseases like diabetic retinopathy [3]. There are various segmentation methods for segmenting the retinal vessels in the fundus image which segments the retinal vessels using two dimensional matched filters and piecewise threshold probing [4, 5]. There are other segmentation processes which include segmentation of retinal vessels using the Mumford-Shah model and Gabor wavelet filter [6]. Extraction of retinal blood vessels is done using Weiner filter and the Morphological operations like open and close operation [7]. This paper focuses on segmentation of the retinal vessels to identify the changes in the retinal vessel which occurs due to retinal pathologies like diabetic retinopathy [8]. Vessel segmentation is done using Max-Tree to represent the image and the branches filtering approach to segment the image [9]. Mathematical morphology is mostly used for analyze the shape of the image. The two main processes which involve are dilation and erosion. The

algorithms of open and close are based on these processes. These algorithms are combined to detect the edges and identifying the specific shapes in the image and also for the background removal [10]. Retinal vessel segmentation is done to classify the pixel as the vessel and non-vessel using morphological thresholding. The retinal blood vessel is extracted by first smoothing the image and enhanced by applying the fuzzy c-means clustering algorithm [11].

2. METHODS

This paper proposes a novel algorithm for retinal blood vessels segmentation. The fundus image used in this research is obtained from two publicly available databases, the DRIVE database [12] and the STARE database [13]. The segmentation of the retinal blood vessel should be automatic and accurate for the diagnosis of the retinal disease. The proposed algorithm and respective details will be explained here.

2.1. Overview of The Proposed Algorithm

The method herein presented can be schematically described by the functional block diagram in Figure 1.

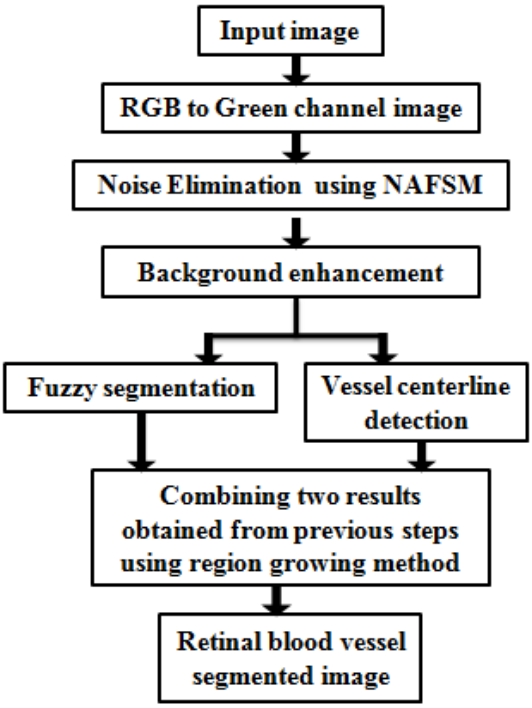

Figure 1. Retinal vessel segmentation functional diagram for the proposed algorithm

The algorithm consists four main parts: 1) preprocessing which includes noise elimination, background normalization and thin vessel enhancement using green channel of the retinal color images 2) processing which includes two phases, vessel centerline detection and Fuzzy vessel segmentation, and 3) Combining two results obtained from previous steps to finally extract the complete pixels belonging to the retinal vessels.

2.2. Image Preprocessing

2.2.1. RGB to Green Channel Conversion

The color fundus image is converted to green channel image to make the segmentation process more easily and to decrease the computational time. The green channel image provides the maximum contrast between the image and the background, because the retinal blood vessel information in the green channel image is more clear [14, 15].

2.2.2. Noise Elimination using Noise Adaptive Fuzzy Switching Median filter (NAFSM)

NAFSM filter is a recursive double-stage filter, where initially it will detect the salt-and-pepper noise intensities before identifying the locations of possible noise pixels. When a "noise pixel" is detected, it is subjected to the next filtering stage. When a pixel is identified as "noise-free," it will be retained and the filtering action is spared to avoid changing any fine details that are contained in the original image.

2.2.2.1. Detection Stage

NAFSM filter will use the noisy image histogram to estimate the two salt-and-pepper noise intensities [16]. The local maximum, which is the first peak encountered when traversing the image histogram in a particular direction, is used [17]. Therefore, the NAFSM filter will search for two local maximums, L_{salt}=255 and L_{pepper}=0, describing the two salt and pepper noise. When both local maximums are found, the search will be stoped immediately. A binary noise mask N(i,j) will be created to show the location of "noise pixels". This mask is shown in Equation 1.

$$N(i,j) = \begin{cases} 0, & X(i,j) = L_{\text{salt}} \text{ or } L_{\text{pepper}} \\ 1, & \text{otherwise} \end{cases} \quad (1)$$

Where X(i,j) is the pixel at location (i,j) with intensity X. N(i,j)=1 represent "noise-free pixels'' to be safed from the noisy image while N(i,j)=0 represents "noise pixels" subjected to the next filtering stage.

2.2.2.2. Filtering Stage

After the binary noise mask N(i,j) is created, "noise pixels" will be replaced by an estimated correction term [18]. NAFSM filter uses a square filtering window W_{2s+1}(i,j) with odd (2s+1)×(2s+1) dimentions, given as Equation 2.

$$W_{2s+1}(i,j) = \{X(i+m, j+n)\} \text{ where } m,n \in (-s,\ldots,0,\ldots,s) \quad (2)$$

Then, the number of "noise-free pixels",$G_{2s+1}(i,j)$ in the filtering window W_{2s+1}(i,j) is counted using Equation 3.

$$G_{2s+1}(i,j) = \sum_{m,n\in(-s,\ldots,0,\ldots,s)} N(i+m, j+n) \quad (3)$$

If the current filtering window W_{2s+1}(i,j) does not have a minimum number of one "noise-free pixel" ($G_{2s+1}(i,j) < 1$), then the filtering window will be expanded by one pixel at each of its four sides (i.e.←s+1) [18]. This procedure is repeated until the condition of $G_{2s+1}(i,j) \geq 1$ is occured. For each detected "noise pixel", the size of the filtering window is initialized to 3×3, i.e., s=1 [18]. These "noise-free pixels" will all be used as candidates for selecting the median pixel, M(i,j), given by Equation 4.

$$M(i,j) = \text{median}\{X(i+m, j+n)\} \text{ with } N(i+m, j+n) = 1 \quad (4)$$

This criterion of choosing only "noise-free pixels" is used to avoid selecting a "noise pixel" as the median pixel. However, the number of "noise-free pixels" for selecting the median pixel is also important because a large number of "noise-free pixel" samples will consume higher computing time and also yield an unsuitable median term for restoration [18]. Since the detection of "noise pixels" is based on the detected salt-and-pepper noise intensities L_{salt} and $L_{perpper}$, noise-free pixels may be falsely identified as "noise pixels" at image uniform regions having same intensities as intensities L_{salt} or $L_{perpper}$. Therefore, the filtering window will be expanded continuously and the selected median pixel may be inaccurate to be used as a correction term. Considering this possibility, the search for "noise-free pixels" is stoped when the filtering window has reached a size of 7×7 (or s=3) and no "noise-free pixel" is detected, i.e., $G_7(i,j)$=0. In this case, the first four pixels in the 3×3 filtering window defined by Equation 5 will be used to compute the median pixel M(i,j) in Equation 6:

$$W_3(i,j) = \{X(i+k, j+l)\} \text{ where } k,l \in (-1,0,1) \quad (5)$$

$$M(i,j) = \text{median}\{X(i-1,j-1), X(i,j-1), X(i+1,j-1), X(i-1,j)\}$$
$$\text{when } s = 3 \text{ and } G_7(i,j) = 0 \tag{6}$$

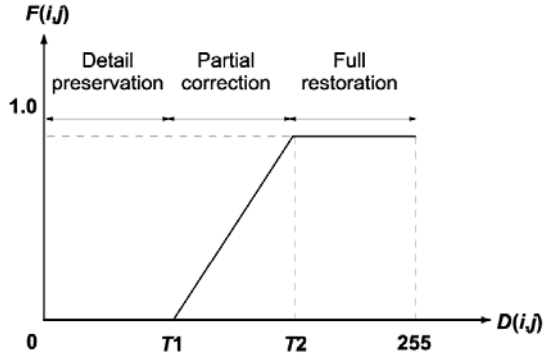

Figure 2. Fuzzy set adapted by the NAFSM filter

The first four pixels chosen, which made up the upper-left diagonal of the 3×3 filtering window, can be justified by the recursive nature of the NAFSM filter. As a result from the recursive behavior, any "noise pixels" in the upper-left diagonal of the 3×3 filtering window would have been restored and updated with "noise-free pixels" during earlier processing. Therefore, using the maximum four "noise-free pixels" in the upper-left diagonal will yield a more accurate median pixel instead of considering all eight connected neighboring pixels.

After the median pixel M(i,j) is found, the local information in a 3×3 window is extracted by first computing the absolute luminance difference d(i,j) as given by Equation 7.

$$d(i+k,j+l) = |X(i+k,j+l) - X(i,j)|$$
$$\text{with } (i+k,j+l) \neq (i,j) \tag{7}$$

Then, the local information is defined as the maximum absolute luminance difference in the 3×3 filtering window by Equation 8.

$$D(i,j) = \max\{d(i+k,j+l)\} \tag{8}$$

As part of the filtering mechanism in the NAFSM filter, fuzzy reasoning is applied to the extracted local information D(i,j) [18]. The fuzzy set adopted is shown in Fig.2 and defined by the fuzzy membership function F(i,j) in Equation 9.

$$F(i,j) = \begin{cases} 0, & : \quad D(i,j) < T_1 \\ \frac{D(i,j)-T_1}{T_2-T_1}, & : \quad T_1 \leq D(i,j) < T_2 \\ 1, & : \quad D(i,j) \geq T_2 \end{cases} \tag{9}$$

where the local information D(i,j) is used as the fuzzy input variable, and the two predefined thresholds T_1 and T_2 are set to 10 and 30, respectively, for optimal performance [17, 18].
Finally, the correction term to restore a detected "noise pixel" is a linear combination between the processing pixel X(i,j) and median pixel M(i,j). The restoration term Y(i,j) is given here as Equation 10.

$$Y(i,j) = [1 - F(i,j)] \cdot X(i,j) + F(i,j) \cdot M(i,j) \tag{10}$$

where the fuzzy membership value F(i,j) leads a weight on whether more of pixel X(i,j) or M(i,j) is to be used.

2.2.3. Background Enhancement

2.2.3.1. Modified Top-hat Transform

The classical top-hat transform is defined as the difference between an image and its opened version. A problem associated with this classical implementation is the sensitivity to noise, as a consequence of the fact that pixel values in an opened image are always less than or equal to the original ones; in such conditions, the different image retains all small intensity fluctuations that can be found in the data. To overcome this problem, a modification was adapted from [19], by considering two new steps in the top-hat definition: a closing precedes the opening result which is followed by a comparison, using a minimum operator, to get an image equal to the original one everywhere except for peaks and ridges. Equation (11) represents this modified top-hat transform, where I is the image to be processed, while Sc and So stand for the structuring elements for closing(•) and opening (***o***) operators, respectively[20].

$$TopHat= I - \min (I\bullet Sc) \boldsymbol{o} So ; I) \quad (11)$$

The closing operation is considered to generate a smooth version of the original data, where the details smaller than the structuring element are replaced by higher nearby intensities. The opened image essentially maintains the pixel values, while eliminating more intense image regions with sizes smaller than the structuring element size. The final result of the subtraction is an enhanced image that mostly retains the original image regions with size smaller than the structuring element which show significant local intensity variations.

Here we propose the modified Top-hat transform to produce the background normalized image. Figure 3(b) presents the background normalized image obtained with the modified top-hat operator. Since thin vessels are very small structures and usually have low local contrast, their segmentation is a hard task. Therefore, it is necessary to deepen the contrast of these images to provide a better transform representation for subsequent image analysis steps. CLAHE technique is adopted to perform the contrast enhancement. This technique enhances the contrast adaptively across the image by limiting the maximum slope in the transformation function. Figure 3(c) presents the vessel enhanced image obtained with the CLAHE technique.

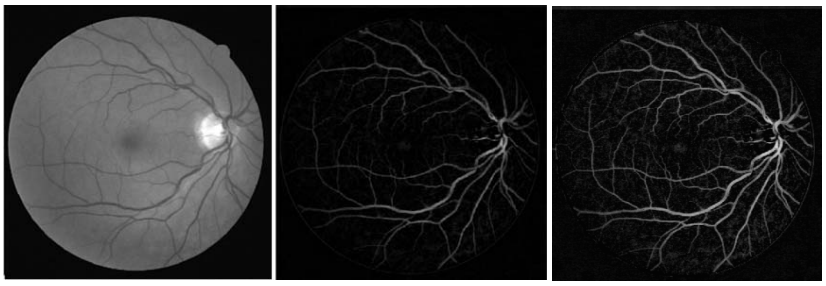

a b c

Figure 3. a) Original green channel b) Background normalized image c) Vessel enhanced image

2.3. Image Processing

2.3.1. Detection of Vessel Centerline

When a first-order derivative filter is applied orthogonally to the main orientation of the vessel, derivative values with opposite signs are created on the two vessel hillsides. This idea is shown in Figure 4(a) for an ideal vessel cross profile.

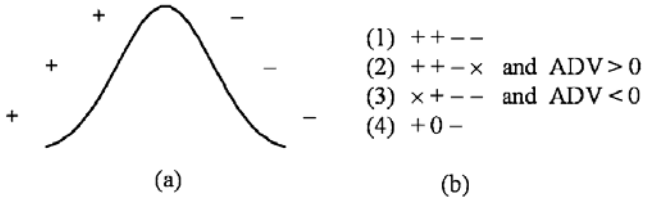

Figure 4. Ideal vessel profile with expected derivative signs on opposite hillsides. (b) Combinations of derivative signs and average derivative values that calculate the occurrence of a candidate centerline point: + means a positive derivative value;—means a negative value; 0 means a zero value; × is a do not care condition; ADV is the mean value of the derivative magnitudes obtained for the same set of four pixels were the specific combination of signs occurred.

As retinal vessels exist in any direction, we need to select a set of directional filters whose responses can be combined to cover the whole range of possible orientations. The particular kernels used in this work are first-order derivative filters, with common responses to horizontal (0), vertical (90), and diagonal (45,135) directions. These filters are used for the computation of the local image gradient in a specific direction.

Herein, the proposed filters used for detecting centerline candidate pixels and the result of applying these filters are shown in Figure 5 and 6 respectively.

$$\begin{bmatrix} 0 & -1 & -2 & -1 & 0 \\ -1 & -2 & -4 & -2 & -1 \\ 0 & 0 & 0 & 0 & 0 \\ 1 & 2 & 4 & 2 & 1 \\ 0 & 1 & 2 & 1 & 0 \end{bmatrix} \begin{bmatrix} 0 & -1 & -2 & -1 & 0 \\ -1 & -4 & -2 & 0 & 1 \\ -2 & -2 & 0 & 2 & 2 \\ -1 & 0 & 2 & 4 & 1 \\ 0 & 1 & 2 & 1 & 0 \end{bmatrix} \begin{bmatrix} 0 & -1 & 0 & 1 & 0 \\ -1 & -2 & 0 & 2 & 1 \\ -2 & -4 & 0 & 4 & 2 \\ -1 & -2 & 0 & 2 & 1 \\ 0 & -1 & 0 & 1 & 0 \end{bmatrix} \begin{bmatrix} 0 & 1 & 2 & 1 & 0 \\ -1 & 0 & 2 & 4 & 1 \\ -2 & -2 & 0 & 2 & 2 \\ -1 & -4 & -2 & 0 & 1 \\ 0 & -1 & -2 & -1 & 0 \end{bmatrix}$$

Figure 5. The proposed filters

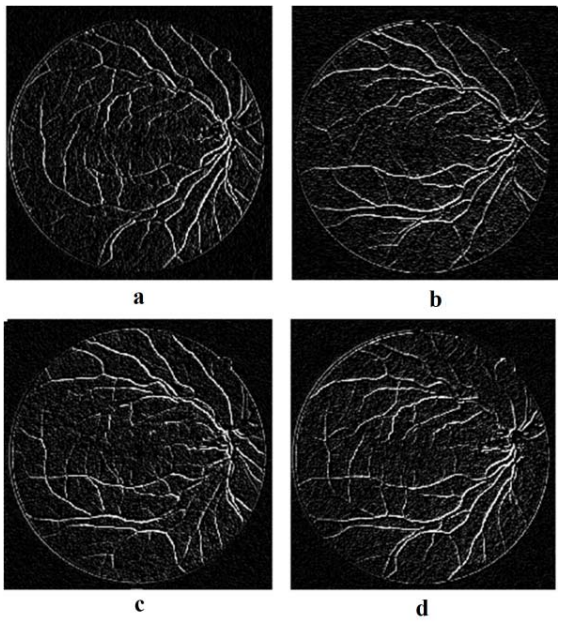

Figure 6. The candidate centerline pixels by applying the proposed filters:
a) vertical b) horizontal c) 135 d) 45.

Each one of the four directional images resulting from the proposed filters is searched for specific combinations of signs on the expected direction of the vessel cross section [20]; Since real vessels do not have the ideal profile presented in Figure 4(a), a set of four combinations represented in Figure 4(b) that can find a vessel are used. In this figure, plus and minus signs show the positive and negative derivative responses, respectively, 0 means a null output, and × shows a do not care condition for the sign of the derivative. Moreover, in conditions 2 and 3, the average value of the derivative magnitudes (ADV) for the intensity profile is calculated. It must be positive for condition 2, and negative for condition 3. The final centerline candidate is simply the pixel with the maximum intensity in the background normalized image [20]. This fact is obtained in a new image by applying the sum of the highest positive response with the absolute value of the most negative response.

Upto here, we could achieve vessel centerlines in retinal images. This method can fully extract the vessel centers, but not the actual width of the vessels.

2.3.2. Fuzzy Segmentation

With the aim of achieving a complete segmentation, retinal vessels need to be filled starting from the detected centerlines. For this purpose, we propose a fuzzy approach which uses fuzzy C-means clustering technique to generate representation of the retinal vascular network with actual width of the vessels. We apply the fuzzy C-means clustering to the vessel enhanced image obtained from preprocessing step.

2.3.2.1. Fuzzy C-means (FCM)

In pattern recognition a clustering method known as Fuzzy C-Means (FCM) is widely used. FCM based segmentation is fuzzy pixel classification [22]. FCM allows data points or pixels to belong to multiple classes with varying degree of membership function between 0 to 1. FCM possesses precious advantage of grading linguistic variables to fit for appropriate analysis in discrete domain on pro-rata basis. FCM computes cluster centers by minimizing the dissimilarity function using an iterative approach. By updating the cluster centers and the membership grades for each unique pixel, FCM shifts the cluster centers to the "true" location within set of pixels. To accommodate the introduction of fuzzy partitioning, the membership matrix (U) =[uij] is randomly initialized according to Equation 12, where uij being the degree of membership function of the data point of i^{th} cluster xi.

$$\sum_{i=1}^{c} u_{ij} = 1, \forall j = 1,..., n \tag{12}$$

The performance index for membership matrix U and C_i's used in FCM is given by Equation 13.

$$J(U, c_1, c_2, ..., c_c) = \sum_{i=1}^{c} J_i = \sum_{i=1}^{c} \sum_{j=1}^{n} {u_{ij}}^m {d_{ij}}^2 \tag{13}$$

uij is between 0 and 1. ci is the center of cluster i. dij is the Euclidian distance between i^{th} center (ci) and j^{th} data point. m ϵ [1,∞] is a weighting exponent. To reach a minimum of dissimilarity function there are two conditions [22]. These are given in Equation 14 and Equation 15.

$$c_i = \frac{\sum_{j=1}^{n} {u_{ij}}^m x_j}{\sum_{j=1}^{n} {u_{ij}}^m} \tag{14}$$

$$u_{ij} = \frac{1}{\sum_{k=1}^{c} \left(\frac{d_{ij}}{d_{kj}} \right)^{2/(m-1)}} \tag{15}$$

Algorithm of FCM is described as below:
Step 1. The membership matrix (U) that has constraints in Eqn 12 is randomly initialized.
Step 2. Centers (ci) are calculated by using Eqn 14.
Step 3. Dissimilarity between centers and data points using Eqn 13 is computed. Stop if its improvement over previous iteration is below a threshold.

Step 4. A new U using Eqn 15 is computed. Go to Step 2 [22].

The result of applying the FCM algorithm to the vessel enhanced image is shown in Figure 7.

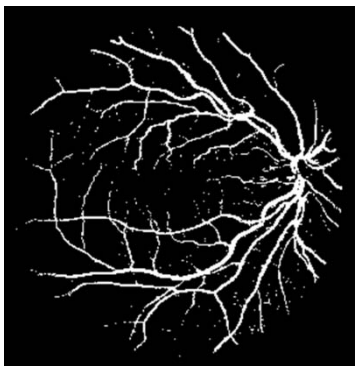

Figure 7. Image resulted from fuzzy segmentation step

Notic that the thin vessels in the fuzzy segmented image are not detected. Therefore, we combine the resulted images from two processing phases, vessel centerline detection and Fuzzy vessel segmentation to achieve a complete vessel segmentation.

2.4. Region Growing

The final image with the segmented vessels is obtained by iteratively combining the centerline images with the image that resulted from the fuzzy segmentation part. Vessel centerline pixels are used as primary points for a region growing algorithm, which fill these points by aggregating the pixels in the fuzzy segmentation image. Final result of the vessel filling part is illustrated in Figure 8.

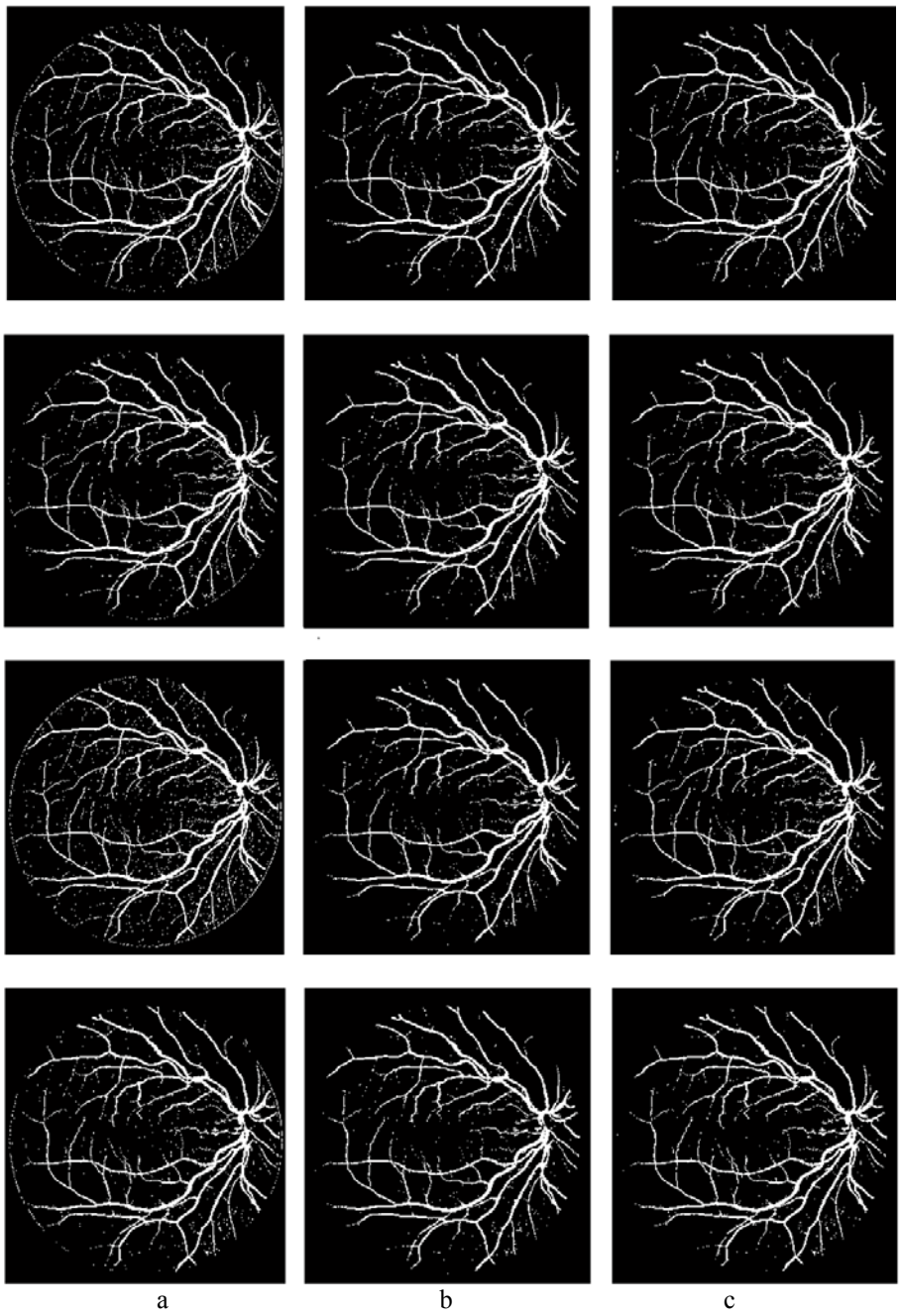

Figure 8. a) Combination of the centerline image with the fuzzy segmented image b) The fuzzy segmented image c) The segmented image using region growing algorithm

At the end, the final segmented image is achieved by adding the four images obtained from the region growing step. Some examples of the segmented images from DRIVE and STARE databases are shown in Figure 9 and Figure 10 respectively.

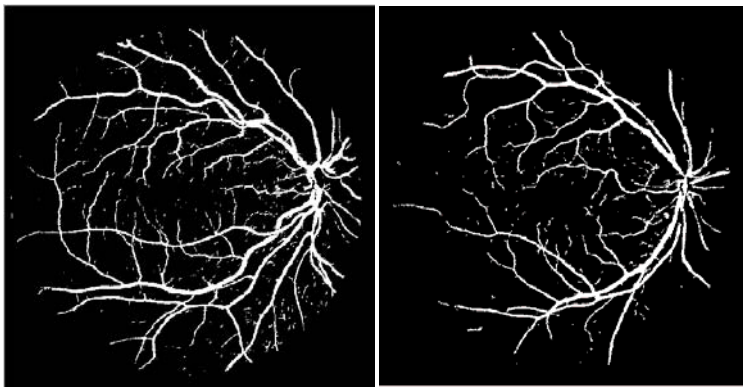

Figure 9. Two examples of segmented images from DRIVE database

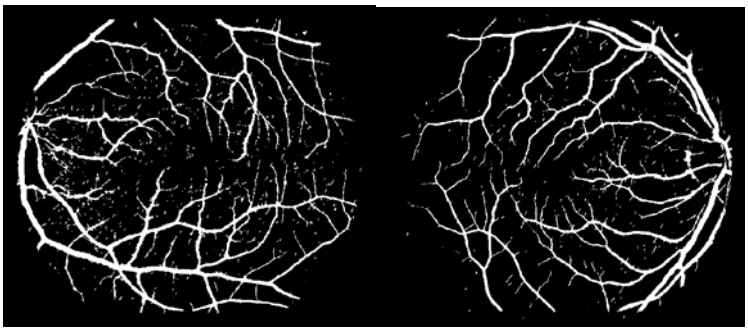

Figure 10. Two examples of segmented images from STARE database

The evaluation results are given as the pixel-wise sensitivity, specificity, and accuracy of all the segmentation in comparison with ground truth, where sensitivity is a normalized measure of true positives, specificity measures the proportion of true negatives, and accuracy represents the proportion of the total number of correctly classified pixels relative to the total number of pixels. In the following equations, true positive (TP) is a number of blood vessels correctly detected, false positive (FP) is a number of non-blood vessels which are detected wrongly as blood vessels, false negative (FN) is a number of blood vessels that are not detected and true negative (TN) is a number of non-blood vessels which are correctly identified as non-blood vessels.

$$\text{Sensitivity} = \frac{TP}{TP+FN}$$

$$\text{Specificity} = \frac{TN}{TN+FP}$$

$$\text{Accuracy} = \frac{(TP+TN)}{(TP+TN+FP+FN)}$$

Table 1 and 2 compares evaluation results of proposed method with the listed approaches on the DRIVE and STARE databases, respectively. Comparisons based on DRIVE database indicate that our proposed method has the highest accuracy, sensitivity and specificity compared to [24]. In addition, it has the highest accuracy and sensitivity compared to [23], [25], [27], [28] and [29]. Moreover, it has the highest accuracy and specificity in comparison with [26].

Comparing the methods on the STARE database illustrate that our proposed method has the highest accuracy, sensitivity and specificity compared to [30], [31] and [5]. In addition, it has the highest accuracy and sensitivity in comparison with [32].

Table 1. Average percentage of proposed method on DRIVE database

method	accuracy	sensitivity	specificity
First proposed method	95.13	72.52	97.33
Baisheng Dai [23]	94.60	70.91	98.06
Espona [24]	93.16	66.34	96.82
Al-Diri [25]	92.58	67.16	_
Vlachos [26]	92.85	74.68	95.51
Fraz [27]	94.30	71.52	97.68
Al-Diri [28]	92.58	67.16	_
Soares [29]	93.16	66.34	96.82

Table 2. Average percentage of proposed method on STARE database

method	accuracy	sensitivity	specificity
First proposed method	95.37	77.66	96.80
Fraz [30]	94.42	73.11	96.80
Zana [31]	93.77	69.71	-
Hoover [5]	92.62	67.51	95.67
Diego Marin1 [32]	95.26	69.44	98.19

3. CONCLUSION

We proposed a retinal blood vessel segmentation method in this paper. This technique is based on vessel centerline detection and fuzzy segmentation. Our proposed vessel extraction technique has consistent performance in both normal and abnormal images. To validate the proposed method we used images provided from two public databases, DRIVE and STARE databases. We could achieve the greatest specificity, accuracy and sensitivity, 95.13, 72.52 and 97.33 for the DRIVE database and 95.37, 77.66 and 96.80 for the STARE database.

REFERENCES

[1] A.K. Jain, *Fundamentals of digital image processing* vol. 3: Prentice-Hall Englewood Cliffs, 1989.
[2] L. Pedersen, M. Grunkin, B. Ersbøll, K. Madsen, M. Larsen, N. Christoffersen, *et al.*, "Quantitative measurement of changes in retinal vessel diameter in ocular fundus images", *Pattern Recognition Letters,* vol. 21, pp. 1215-1223, 2000.
[3] C. Sinthanayothin, J. Boyce, T. Williamson, H. Cook, E. Mensah, S. Lal, *et al.*, "Automated detection of diabetic retinopathy on digital fundus images", *Diabetic Medicine,* vol. 19, pp. 105-112, 2002.
[4] S. Chaudhuri, S. Chatterjee, N. Katz, M. Nelson, and M. Goldbaum, "Detection of blood vessels in retinal images using two-dimensional matched filters", *IEEE Transactions on medical imaging*, vol. 8, pp. 263-269, 1989.
[5] A. Hoover, V. Kouznetsova, and M. Goldbaum, "Locating blood vessels in retinal images by piecewise threshold probing of a matched filter response", *IEEE Transactions on Medical Imaging,* vol. 19, pp. 203-210, 2000.
[6] X. Du and T.D. Bui, "Retinal image segmentation based on Mumford-Shah model and Gabor wavelet filter", in *Pattern Recognition (ICPR), 2010 20th International Conference on*, 2010, pp. 3384-3387.
[7] V.V. Kumari and N. Suriyanarayanan, "Blood vessel extraction using wiener filter and morphological operation", *Int. J. Comput. Sci. Emerg. Technol,* vol. 1, pp. 7-10, 2010.
[8] M. Foracchia, E. Grisan, and A. Ruggeri, "Extraction and quantitative description of vessel features in hypertensive retinopathy fundus images", in *Book Abstracts 2nd International Workshop on Computer Assisted Fundus Image Analysis*, 2001, p. 6.
[9] Y. Yang, S. Huang, and N. Rao, "An automatic hybrid method for retinal blood vessel extraction", *International Journal of Applied Mathematics and Computer Science,* vol. 18, pp. 399-407, 2008.
[10] N. Patton, T.M. Aslam, T. MacGillivray, I.J. Deary, B. Dhillon, R.H. Eikelboom, *et al.*, "Retinal image analysis: concepts, applications and potential", *Progress in retinal and eye research,* vol. 25, pp. 99-127, 2006.
[11] K. Noronha, J. Nayak, and S. Bhat, "Enhancement of retinal fundus Image to highlight the features for detection of abnormal eyes", in *TENCON 2006. 2006 IEEE Region 10 Conference*, 2006, pp. 1-4.
[12] M. Niemeijer, J.J. Staal, B.v. Ginneken, M. Loog, M.D.Abramoff, DRIVE: digital retinal images for vessel extraction, http://www.isi.uu.nl/Research/Databases/DRIVE,2004.
[13] A. Hoover, V. Kouznetsova, and M. Goldbaum, "Locating blood vessels in retinal images by piecewise threshold probing of a matched filter response", *IEEE Transactions on Medical Imaging,* vol. 19, pp. 203-210, 2000.
[14] A. Bouchet, M. Brun, and V. Ballarin, "Morfología Matemática Difusa aplicada a la segmentación de angiografías retinales", *Revista Argentina de Bioingeniería,* vol. 16, pp. 7-10, 2001.
[15] A. Bouchet, J.I. Pastore, and V.L. Ballarín, "Segmentation of medical images using fuzzy mathematical morphology", *Journal of Computer Science & Technology,* vol. 7, 2007.

[16] W. Luo, "Efficient removal of impulse noise from digital images", *IEEE Transactions on Consumer Electronics,* vol. 52, pp. 523-527, 2006.
[17] K.K.V. Toh, H. Ibrahim, and M.N. Mahyuddin, "Salt-and-pepper noise detection and reduction using fuzzy switching median filter", *IEEE Transactions on Consumer Electronics,* vol. 54, pp. 1956-1961, 2008.
[18] K. K. V. Toh and N. A. M. Isa, "Noise adaptive fuzzy switching median filter for salt-and-pepper noise reduction", *IEEE Signal Processing Letters,* vol. 17, pp. 281-284, 2010.
[19] J. Gasparri, A. Bouchet, G. Abras, V. Ballarin, and J. Pastore, "Medical Image Segmentation using the HSI color space and Fuzzy Mathematical Morphology", in *Journal of Physics: Conference Series*, 2011, p. 012033.
[20] A.M. Mendonca and A. Campilho, "Segmentation of retinal blood vessels by combining the detection of centerlines and morphological reconstruction", *IEEE Transactions on Medical Imaging,* vol. 25, pp. 1200-1213, 2006.
[21] W. K. Pratt, *Digital Image Processing*, 3rd ed. New York: Wiley, 2001.
[22] N. Dey, A.B. Roy, M. Pal, and A. Das, "FCM based blood vessel segmentation method for retinal images", *arXiv preprint arXiv:1209.1181,* 2012.
[23] B. Dai, W. Bu, X. Wu, and Y. Teng, "Retinal vessel segmentation via Iterative Geodesic Time Transform", in *Pattern Recognition (ICPR), 2012 21st International Conference on*, 2012, pp. 561-564.
[24] L. Espona, M. J. Carreira, M. Ortega, and M. G. Penedo, "A snake for retinal vessel segmentation", in *Pattern Recognition and Image Analysis*, ed: Springer, 2007, pp. 178-185.
[25] B. Al-Diri, A. Hunter, and D. Steel, "An active contour model for segmenting and measuring retinal vessels", *IEEE Transactions on Medical Imaging,* vol. 28, pp. 1488-1497, 2009.
[26] M. Vlachos and E. Dermatas, "Multi-scale retinal vessel segmentation using line tracking", *Computerized Medical Imaging and Graphics,* vol. 34, pp. 213-227, 2010.
[27] M.M. Fraz, P. Remagnino, A. Hoppe, B. Uyyanonvara, C.G. Owen, A.R. Rudnicka*, et al.*, "Retinal vessel extraction using first-order derivative of Gaussian and morphological processing", in *Advances in Visual Computing*, ed: Springer, 2011, pp. 410-420.
[28] B. Al-Diri, A. Hunter, and D. Steel, "An active contour model for segmenting and measuring retinal vessels", *IEEE Transactions on Medical Imaging,* vol. 28, pp. 1488-1497, 2009.
[29] J.V. Soares, J.J. Leandro, R.M. Cesar, H.F. Jelinek, and M.J. Cree, "Retinal vessel segmentation using the 2-D Gabor wavelet and supervised classification", *IEEE Transactions on Medical Imaging,* vol. 25, pp. 1214-1222, 2006.
[30] M.M. Fraz, S. Barman, P. Remagnino, A. Hoppe, A. Basit, B. Uyyanonvara*, et al.*, "An approach to localize the retinal blood vessels using bit planes and centerline detection", *Computer methods and programs in biomedicine,* vol. 108, pp. 600-616, 2012.
[31] F. Zana and J.C. Klein, "A multimodal registration algorithm of eye fundus images using vessels detection and Hough transform", *IEEE Transactions on Medical Imaging,* vol. 18, pp. 419-428, 1999.
[32] D. Marín, A. Aquino, M.E. Gegúndez-Arias, and J.M. Bravo, "A new supervised method for blood vessel segmentation in retinal images by using gray-level and moment invariants-based features", *IEEE Transactions on Medical Imaging,* vol. 30, pp. 146-158, 2011.

BIOGRAPHIES OF AUTHORS

Razieh Akhavan, received her B.S. degree in software of computer Engineering from Lahijan Azad University as the first rank in May 2010, and now the student of M.S. degrees in Artificial Intelligence of Computer Science from Electrical and Computer Engineering Department of Islamic Azad University of Qazvin, Iran. Her research interests are in Pattern Recognition, Biometric Identification and Recognition, Image Processing, Neural Networks, Signal Processing, Farsi Handwritten Recognition.
Email: R.akhavan.a@gmail.com.

Karim Faez, received his B.S. degree in Electrical Engineering from Tehran Polytechnic University as the first rank in June 1973, and his M.S. and Ph.D. degrees in Computer Science from University of California at Los Angeles (UCLA) in 1977 and 1980, respectively. Prof. Faez was with Iran Telecommunication Research Center (1981-1983) before joining Amirkabir University of Technology in Iran. He was the founder of the Computer Engineering Department of Amirkabir University in 1989 and he has served as the first chairman during April 1989-Sept. 1992. Professor Faez was the chairman of planning committee for Computer Engineering and Computer Science of Ministry of Science, research and Technology (during 1988-1996). His research interests are in Pattern Recognition, Biometric Identification and Recognition, Image Processing, Steganography, Neural Networks, Signal Processing, Farsi Handwritten Recognition, Earthquake Signal Processing, Fault Tolerant System Design, Computer Networks. He is a member of IEEE, IEICE, and ACM. Emails: kfaez@aut.ac.ir, kfaez@ieee.org.